



1 **Dynamics of transparent exopolymer particles (TEP) during**
2 **the VAHINE mesocosm experiment in the New Caledonia**
3 **lagoon**

4

5 **I. Berman-Frank¹, D. Spungin¹, E. Rahav^{1,2}, F. Van Wambeke³, K. Turk-Kubo⁴, T.**
6 **Moutin³**

7 [1] Mina and Everard Goodman Faculty of Life Sciences, Bar-Ilan University, Ramat Gan,
8 Israel 5290002

9 [2] National Institute of Oceanography, Israel Oceanographic and Limnological Research,
10 Haifa, Israel

11 [3] Aix Marseille Université, CNRS/INSU, Université de Toulon, IRD, Mediterranean
12 Institute of Oceanography (MIO) UM110, 13288, Marseille, France

13 [4] Ocean Sciences Department, University of California, Santa Cruz, 1156 High Street, Santa
14 Cruz, CA, 95064, USA

15

16 Correspondence to: I. Berman-Frank (ilana.berman-frank@biu.ac.il)

17

18

19

20

21

22

23

24

25

26



27 **Abstract**

28 In the marine environment, transparent exopolymeric particles (TEP) produced from abiotic
29 and biotic sources link the particulate and dissolved carbon pools and are essential vectors
30 enhancing vertical carbon flux. We characterized spatial and temporal dynamics of TEP
31 during the VAHINE experiment that investigated the fate of diazotroph derived nitrogen and
32 carbon in three, replicate, dissolved inorganic phosphorus (DIP)-fertilized 50 m³ enclosures in
33 an oligotrophic New Caledonian lagoon. During the 23 days of the experiment, we did not
34 observe any depth dependent changes in TEP concentrations in the three sampled-depths (1,
35 6, 12 m). TEP carbon (TEP-C) content per mesocosm averaged $28.9 \pm 9.3\%$ and $27.0 \pm 7.2\%$
36 of TOC in the mesocosms and surrounding lagoon respectively and was strongly and
37 positively coupled with TOC during P2. TEP concentrations declined for the first 9 days after
38 DIP fertilization (P1 = days 5-14) and then gradually increased during the second phase (P2 =
39 days 15-23). Temporal changes in TEP concentrations paralleled the growth and mortality
40 rates of the diatom-diazotroph association of *Rhizosolenia* and *Richelia* that predominated the
41 diazotroph community during P1. By P2, increasing total primary and heterotrophic bacterial
42 production consumed the supplemented P and reduced availability of DIP. For this period,
43 TEP concentrations were negatively correlated with DIP availability and turnover time of DIP
44 (T_{DIP}) while positively associated with enhanced alkaline phosphatase activity (APA) that
45 occurs when the microbial populations are P-stressed. During P2, increasing bacterial
46 production (BP) was positively correlated with higher TEP concentrations which were also
47 coupled with the increased growth rates and aggregation of the unicellular UCYN-C
48 diazotrophs which bloomed during this period. We conclude that the composite processes
49 responsible for the formation and breakdown of TEP yielded a relatively stable TEP pool
50 available as both a carbon source and facilitating aggregation and flux throughout the
51 experiment. TEP was probably mostly influenced by abiotic physical processes during P1
52 while biological activity (BP, diazotrophic growth and aggregation, export production) mainly
53 impacted TEP concentrations during P2 when DIP-availability was limited.

54

55 **1 Introduction**

56 The cycling of carbon (C) in the oceans is a complex interplay between physical,
57 chemical, and biological processes that regulate the input and the fate of carbon within the
58 ocean. An essential process driving the flux of carbon and other organic matter to depth and
59 enabling long term sequestration and removal of carbon from the atmosphere is the biological



60 pump that drives organic C formed during photosynthesis to the deep ocean. This process,
61 termed export production (Eppley and Peterson, 1979), is facilitated via physical inputs of
62 ‘new’ nutrients (e.g. nitrogen, phosphorus, silica, trace metals, etc.) into the euphotic zone
63 from either external sources (deep mixing of upwelled water, river discharge, dust deposition,
64 and anthropogenic inputs) or via biological processes such as microbial N_2 fixation that
65 converts biologically unavailable dinitrogen (N_2) gas into bioavailable forms of nitrogen and
66 enhances the productivity of oligotrophic oceanic surface waters that are often limited by
67 nitrogen (Falkowski, 1997; Capone, 2001).

68 Marine N_2 fixation is performed by diverse prokaryotic organisms comprised
69 predominantly of autotrophic cyanobacteria and heterotrophic bacteria (Zehr and Kudela,
70 2011). To supply the energetically-expensive process of converting N_2 to ammonia (Stam et
71 al., 1987; Postgate and Eady, 1988; Mulholland and Capone, 2000), these organisms must
72 obtain energy from either photosynthesis (cyanobacteria) or from bioavailable organic carbon
73 compounds within the aquatic milieu (heterotrophic bacteria and mixotrophs). The total
74 organic carbon (TOC) in the ocean contains dynamic particulate (POC) and dissolved organic
75 carbon (DOC) pools that are supplied by biotic sources that are broken down into organic C-
76 containing marine microgels which include transparent polymeric particles (TEP). TEP are
77 predominantly acidic polysacchridic organic particles ranging in size from ~ 0.45 to $> 300 \mu\text{m}$
78 and are found in both marine and freshwater habitats (Passow, 2002). Both biotic and abiotic
79 processes form aquatic TEP that are routinely detected by staining with Alcian Blue
80 (Alldredge et al., 1993; Passow and Alldredge, 1995). Abiotic TEP occur by coagulation of
81 colloidal precursors in the pool of dissolved organic matter (DOM) and from planktonic
82 debris (Passow, 2002; Verdugo and Santschi, 2010) that may be stimulated by turbulence or
83 by bubble adsorption (Logan et al., 1995; Zhou et al., 1998; Passow, 2002). Biotically TEP
84 form from extracellular excretion or mucilage in algae and bacteria and from grazing and
85 microbial breakdown of larger marine snow particles [reviewd in (Passow, 2002; Bar-Zeev et
86 al., 2015)].

87 TEPs are light and bouyant (Azetsu-Scott and Passow, 2004). Yet, once formed, TEPs
88 sticky nature enhances and consolidates the formation of larger aggregates such as
89 marine/lake snow providing favorable environments for diverse microorganisms (Passow,
90 2002; Engel, 2004). Sedimentation of TEP associated “hot spots” from the surface are
91 important for transporting particulate organic material and microorganisms to deeper waters
92 (Smith and Azam, 1992; Azam and Malfatti, 2007; Bar-Zeev et al., 2009). During



93 sedimentation, TEP can also function as a direct source of carbon and other nutrients for
94 higher trophic level organisms such as protists, micro-zooplankton, and nekton (Passow,
95 2002; Engel, 2004).

96 TEP production can be enhanced in late phases of algal blooms and in senescent or
97 nutrient-stressed phytoplankton (Grossart et al., 1997; Passow, 2002; Engel, 2004;
98 Berman-Frank et al., 2007). Thus, TEP in oligotrophic waters (Engel, 2004) provide a source
99 of available carbon to fuel microbial food webs (Azam and Malfatti, 2007) that typically
100 succeed autotrophic blooms. TEP based aggregates or marine snow containing TEP typically
101 with high carbon (C): nitrogen (N) ratios (Wood and Van Valen, 1990; Berman-Frank and
102 Dubinsky, 1999), which can also fuel N₂ fixation by heterotrophic diazotrophs both in
103 oxygenated surface waters and in the aphotic zones (Rahav et al., 2013; Benavides et al., in
104 press).

105 The VAHINE project was designed to examine the fate/s of ‘newly’-fixed N by
106 diazotrophs or diazotroph-derived N (hereafter called DDN) in the pelagic food web using
107 large mesocosms in the oligotrophic tropical lagoon of New Caledonia where diverse
108 diazotrophic populations have been observed (Dupouy et al., 2000; Garcia et al., 2007; Rodier
109 and Le Borgne, 2008; Biegala and Raimbault, 2008; Rodier and Le Borgne, 2010; Bonnet et
110 al., This issue-b). One of the major questions addressed during VAHINE was whether
111 diazotroph blooms significantly modify the stocks, fluxes, and ratios of biogenic elements (C,
112 N, P, Si) and the efficiency of carbon export. To this end, the 3 large-volume (~50 m³)
113 mesocosms containing ambient lagoon waters were fertilized with 0.8 μM DIP, and multiple
114 parameters were measured inside and outside of the mesocosms for 23 days (details of
115 parameters and experimental setup in (Bonnet et al., This issue-b). Within the VAHINE
116 framework, our specific objectives were: 1) to examine the spatial and temporal dynamics of
117 TEP; 2) to determine whether TEP content was regulated by nutrient status in the mesocosms
118 - specifically DIP availability; 3) to examine the relationship between TEP content, particulate
119 and dissolved carbon, and primary or heterotrophic bacterial production; and 4) to elucidate
120 whether TEP provided a source of energy for diazotrophs/bacteria/mixotrophs in mesocosms.

121

122 **2 Methods**

123 **2.1 Study site, mesocosm description, and sampling strategy**

124 Three large-volume (~50 m³) mesocosms were deployed at the exit of the oligotrophic
125 New Caledonian lagoon (22°29.10 S–166°26.90 E), from 13 January 2013 (day 1) to 4



126 February 2013 (day 23). The complete description of the mesocosm design and deployment,
127 as well as sampling strategy is detailed in Bonnet et al. (This issue-b). The mesocosms were
128 intentionally supplemented with $0.8 \mu\text{mol KH}_2\text{PO}_4$ (hereafter referred to as DIP fertilization)
129 between day 4 and 5 day of the experiment to promote N_2 fixation. Samples were collected
130 during the early morning of each day for 23 days with a clean Teflon pumping system from 3
131 selected depths (1 m, 6 m, 12 m) in each mesocosm (M1, M2 and M3) and outside (hereafter
132 called ‘lagoon waters’-O). Based on the results of different biogeochemical and biological
133 parameters during VAHINE (Turk-Kubo et al., 2015; Berthelot et al., 2015; Bonnet et al.,
134 This issue-a), three specific periods were discerned within which we have also investigated
135 TEP dynamics: Days 2-4 (P0) are the pre-fertilization days; days 5-14 (P1), and days 15-23
136 (P2).

137 **2.2 TEP quantification**

138 Water samples (100 mL) were gently (< 150 mbar) filtered through a $0.45 \mu\text{m}$
139 polycarbonate filters (GE Water & Process Technologies). Filters were then stained with a
140 solution of 0.02% Alcian Blue (AB) and 0.06% acetic acid (pH of 2.5). The excess dye was
141 removed by a quick deionized water rinse. Filters were then immersed in sulfuric acid (80%)
142 for 2 h, and the absorbance at 787 nm was measured spectrophotometrically (CARY 100,
143 Varian). AB was calibrated using a purified polysaccharide GX (Passow and Alldredge,
144 1995). TEP concentrations ($\mu\text{g gum xanthan [GX] equivalents L}^{-1}$) were measured according
145 to (Passow and Alldredge, 1995). Total TEP content in the mesocosms was calculated by
146 integrating the weighted average of the TEP concentrations per depth and multiplying by the
147 specific volume of each mesocosm. To estimate the role of TEP in C cycling, total amount of
148 TEP-C was calculated for each mesocosm, using the volumetric TEP concentrations at each
149 depth, the specific volume per mesocosm, and the conversion of GX equivalents to carbon
150 applying the revised factor of 0.63 based on empirical experiments from both natural samples
151 from different oceanic areas and phytoplankton cultures (Engel, 2004).

152 **2.3 TOC, POC, DOC**

153 Samples for total organic carbon (TOC) concentrations were collected in duplicate from
154 6 m in each mesocosm and in lagoon waters in precombusted sealed glassware flasks,
155 acidified with H_2PO_4 and stored in the dark at 4°C until analysis. Samples were analyzed on a
156 Shimadzu TOCV analyzer with a typical precision of $2 \mu\text{mol L}^{-1}$. Samples for particulate
157 organic carbon (POC) concentrations were collected by filtering 2.3 L of seawater through a



158 precombusted GF/F filter (450 °C for 4 h), combusted and analyzed on an EA 2400 CHN
159 analyzer. Dissolved organic carbon (DOC) concentrations were calculated as the difference
160 between TOC and POC concentrations. Fully detailed methodologies and data are available in
161 Berthelot et al. (2015).

162 **2.4 Dissolved inorganic phosphorus (DIP) and alkaline phosphatase activity** 163 **(APA)**

164 The determination of DIP concentrations are detailed in Berthelot et al. (2015). Samples
165 for DIP were collected from each of the three depths in M1, M2 and M3 and lagoon waters
166 (O) in 40 mL glass bottles, and stored in -20 °C until analysis. DIP concentration was
167 determined using a segmented flow analyzer according to (Aminot and K erouel, 2007). The
168 alkaline phosphatase activity (APA) was measured from the same depths and sites using the
169 analog substrate methylumbelliferone phosphate (MUF-P, 1 μM final concentration;
170 SIGMA), (Hoppe, 1983). Full details of the measurements and analyses are described in Van
171 Wambeke et al. (This issue).

172 **2.5 Chlorophyll a (Chl a), Primary production (PP) and DIP turnover time**

173 Chlorophyll a (Chl *a*) concentrations were determined by fluorimetry and the detailed
174 methodologies also for primary production are described in Berthelot et al. (2015). Briefly,
175 primary production (PP) rates and DIP turnover time (T_{DIP} , i.e., the ratio of PO_4^{-3}
176 concentration and uptake) were measured using the $^{14}\text{C}/^{33}\text{P}$ dual labeling method (Duhamel et
177 al., 2006). 60 mL bottles were amended with ^{14}C and ^{33}P and incubated for 3 to 4 h. This was
178 followed by the addition of 50 μL of KH_2PO_4 solution (10 mmol L^{-1}) to stop ^{33}P assimilation.
179 Samples were kept in the dark to stop ^{14}C uptake. Samples were filtered on 0.2 μm
180 polycarbonate membrane filters, and counts were done using a Packard Tri-Carb® 2100TR
181 scintillation counter. PP and T_{DIP} were calculated according to (Moutin et al., 2002).

182 **2.6 Bacterial production (BP)**

183 Heterotrophic bacterial production (BP) was estimated using the ^3H -leucine
184 incorporation technique (Kirchman, 1993), adapted to the centrifuge method (Smith and
185 Azam, 1992). The complete methodology including enumeration of heterotrophic bacterial
186 abundances (BA) by flow cytometry is detailed in Van Wambeke et al. (This issue).



187 **2.7 N₂ fixation, diazotrophic abundance and growth rates**

188 N₂ fixation rates were determined daily on ambient waters from mesocosms and the
189 lagoon. Samples were spiked with 99% ¹⁵N₂-enriched seawater, incubated in-situ under
190 ambient light and seawater temperatures as detailed in Berthelot et al. (2015) and (Bonnet et
191 al., This issue-a).

192 Data and protocols of sampling for diazotrophic abundance and calculation of their
193 respective growth rates are detailed fully in Turk-Kubo et al. (2015). Briefly, samples (from 6
194 m only) were collected every other day from the mesocosms, and from the lagoon waters.
195 DNA was extracted and nine diazotrophic phylotypes were identified using quantitative PCR
196 (qPCR). The targeted diazotrophs were two unicellular diazotrophic symbionts of different
197 *Braarudosphaera bigelowii* strains, UCYN-A1, UCYN-A2; free-living unicellular diazotroph
198 cyanobacterial phylotypes UCYN-B (*Crocospaera* sp.), and UCYN-C (*Cyanothece* sp. and
199 relatives); *Trichodesmium* spp.; and three diatom-diazotroph associations (DDAs), *Richelia*
200 associated with *Rhizosolenia* (Het-1), *Richelia* associated with *Hemiaulus* (Het-2), *Calothrix*
201 associated with *Chaetoceros* (Het-3), and a widespread gamma-proteobacterial phylotype γ-
202 24774A11. Abundances are reported as *nifH* copies L⁻¹ as the number of *nifH* copies per
203 genome in these diazotrophs are uncertain. Growth and mortality rates were calculated for
204 individual diazotrophs inside the mesocosms when abundances were higher than the limit of
205 quantification (LOQ) for two consecutive sampling days as detailed in Turk-Kubo et al.
206 (2015).

207 **2.8 Microscopic Analyses**

208 Detailed method for sampling for microscopic analyses is described in Bonnet et al.
209 (This issue). Phytoplankton were visualized using a Zeiss Axioplan (Zeiss, Jena, 6 Germany)
210 epifluorescence microscope fitted with a green (510-560 nm) excitation filter, which targeted
211 the *Richelia* and the UCYN phycoerythrin-rich cells. The diatom-diazotroph association
212 *Rhizosolenia-Richelia* were imaged in bright-field.

213 **2.9 Statistical analyses**

214 Statistical analyses were carried out with XLSTAT, a Microsoft Office Excel based
215 software. A Pearson correlation coefficient test was applied to examine the association
216 between two variables (TEP versus physical, chemical, or physiological variable) after linear
217 regressions or log-transformation of the data. The non-parametric Kruskal–Wallis one-way



218 analysis of variance was applied to compare between TEP dynamics from each of the
219 different phases. A confidence level of 95% (α - 0.05) was used.

220

221 **3 Results and Discussion**

222 **3.1 General context and spatial and temporal dynamics of TEP**

223 The VAHINE experiment was designed to induce and follow diazotrophic blooms and
224 their fate within an oligotrophic environment (Bonnet et al., This issue-b). Our specific
225 objectives of investigating TEP dynamics were thus examined within the general context and
226 aims of the large experiment. The first stage of the experiment involved the enclosure of the
227 lagoon waters and 3 days of equilibration of the system (P0 – pre-fertilization days 2-4). At
228 this initial stage the total Chl *a* concentrations averaged around 0.2 $\mu\text{g L}^{-1}$ in the lagoon water
229 and in the mesocosms and the phytoplankton consisted of diverse representatives from the
230 cyanobacteria (*Prochlorococcus*, *Synechococcus*, diatoms such as *Pseudosolenia calcar-avis*,
231 and dinoflagellates (Leblanc et al., This issue). During P0, the most abundant members of the
232 diazotrophic community in the lagoon waters were *Richelia-Rhizosolenia* (Het-1), the
233 unicellular UCYN-A1, UCYN-A2, UCYN-C, and the filamentous *Trichodesmium* (Turk-
234 Kubo et al., 2015).

235 Fertilization of the mesocosms with DIP on day 4 stimulated a two-stage response by
236 the diazotrophic community that was further reflected by many of the measured chemical and
237 biological parameters (Berthelot et al., 2015; Turk-Kubo et al., 2015; Bonnet et al., This
238 issue-a; Bonnet et al., This issue-b). After fertilization, from day 5 through day 14 (P1),
239 excluding a significant increase in N_2 fixation rates, the functional community-wide
240 biological responses (Chl *a*, PP, BP, BA) remained relatively low and similar to the values for
241 P0 and for P1 in the outside lagoon waters (Berthelot et al., 2015; Leblanc et al., This issue;
242 Van Wambeke et al., This issue). The autotrophic community during P1 was comprised of
243 picophytoplankton such as *Prochlorococcus*, and *Synechococcus*, micro and
244 nanophytoplankton including dinoflagellates, and a diverse diatom community (*Chaetoceros*,
245 *Leptocylindrus*, *Cerataulina*, *Guinardia*, and *Hemiaulus*), (Leblanc et al., This issue). Diatom-
246 diazotroph associations (DDAs), predominantly *Richelia-Rhizosolenia* (Het-1) dominated the
247 diazotroph community in the mesocosms (Turk-Kubo et al., 2015) although it still only
248 contributed from 2% to ~8% of the total diatom biomass in P0 and P1 respectively (Leblanc
249 et al., This issue). These DDAs were succeeded during the last 9 days (day 15 to 23 termed



250 P2) by a large bloom of unicellular diazotrophs characterized predominantly as UCYN-C
251 (Turk-Kubo et al., 2015).

252 The final stage of the experiment (P2, days 15-23) was characterized by significantly
253 enhanced values for many biological parameters including N_2 fixation rates, Chl *a*, PP, BA,
254 BP, and particulate organic carbon and nitrogen compared to their respective average values
255 in P1 (Leblanc et al., This issue; Van Wambeke et al., This issue; Bonnet et al., This issue-a).
256 In all three mesocosms, a significant bloom of UCYN-C developed (day 11 – M1, day 13-M2,
257 day 15-M3) and remained dominant representatives of the diazotroph community until day
258 23(Turk-Kubo 2015). The ambient autotrophic community responded to the input of new N,
259 and the transfer of diazotroph derived N was demonstrated and seen in increasing abundance
260 of *Synechococcus*, pico-eukaryotes, and the non-diazotrophic diatoms *Navicula* and
261 *Chaetoceros* spp. (Leblanc et al., This issue; Van Wambeke et al., This issue; Bonnet et al.,
262 This issue-a). Thus the extremely high N_2 fixation rates during this experiment provided
263 sufficient new N to yield high Chl *a* concentrations ($> 1.4 \mu\text{g L}^{-1}$) and rates of PP ($>2 \mu\text{mol C}$
264 $\text{L}^{-1} \text{d}^{-1}$)(Berthelot et al., 2015).

265 3.1.1 Dynamics of TEP

266 TEP concentrations for the entire experimental period ranged from ~22 to $1200 \mu\text{g GX}$
267 L^{-1} . In each mesocosm and also in the lagoon waters (O), the TEP concentrations were similar
268 for the three sampled depths within the 15 m water-column with an overall average of $350 \pm$
269 $180 \mu\text{g GX L}^{-1}$ (Fig. S1). Temporally, TEP concentrations generally followed the three
270 distinct periods (P0, P1, P2) that coincided with the described experimental phases
271 characterized from the diazotrophic populations and the biogeochemical and biological
272 (production) parameters (Berthelot et al., 2015; Turk-Kubo et al., 2015; Leblanc et al., This
273 issue; Van Wambeke et al., This issue; Bonnet et al., This issue-a), (Fig. 1, Fig. S1).
274 Following the enclosure of the lagoon water in the mesocosms (day 2), TEP concentrations
275 increased from the lowest volumetric concentrations (averaging~ $50 \mu\text{g GX L}^{-1}$) measured on
276 day 2 to reach maximum concentrations in each of the mesocosms (average of ~ $800 \mu\text{g GX L}^{-1}$)
277 on day 5, ~15 h after the mesocosms were fertilized with DIP (Fig. S1, Fig. 1a). From day 5
278 to day 14 (P1) average TEP content in M2 and M3 decreased slightly yet significantly ($p <$
279 0.05) with the major decline in all mesocosms measured from day 5 to 6 (Fig. 1, Fig. S1,
280 Table S1). From day 15 to 23 (P2) TEP concentrations in all mesocosms increased gradually



281 (p < 0.05) over the subsequent 9 days to reach $381 \pm 39 \mu\text{g GX L}^{-1}$ on day 23 (Fig. 1, Table
282 S1).

283 TEP concentrations in the lagoon waters were compared with those in the mesocosms.
284 These showed a similar pattern of increase in TEP during P0 and P3 while the gradual decline
285 in TEP concentrations during P2 was not statistically significant as observed in the
286 mesocosms (Fig. 1, Fig. S1). In the lagoon waters average TEP concentrations over the whole
287 experimental period day 2 to day 23 were $335 \pm 56 \mu\text{g GX L}^{-1}$. While temporal variations in
288 the three mesocosms were mostly statistically significant (Fig. 1, Table S1), the total TEP
289 content calculated for each mesocosm and for an equivalent volume of lagoon water based on
290 average mesocosm volume) did not differ significantly when we assessed all data obtained
291 during P1 and P2 (Fig. 2, p > 0.05, Kruskal–Wallis analyses of variance). The lack of
292 significant differences in total TEP content in the mesocosms throughout the experiment
293 could reflect the contrasting processes of formation and breakdown that together maintain a
294 relatively stable pool of available TEP.

295 Mechanical processes such as wave turbulence and tidal effects can influence TEP
296 formation and breakdown (and resulting content), (Stoderegger and Herndl, 1999; Passow,
297 2002). Our results indicate no obvious effects of these parameters on TEP content as these
298 were similar in the enclosed mesocosms and the outside lagoon (Fig. 1, Fig. 2). Moreover,
299 despite the initial increase in mesocosm TEP concentrations prior to DIP fertilization, and for
300 the first 15 h after fertilization, from day 5 to the end of the experiment, TEP concentrations
301 were similar for both DIP-fertilized mesocosms and the lagoon waters with low DIP
302 concentrations (Fig. 1, Fig. S1, Fig. 2). This implies that also DIP fertilization had no impact
303 on the resulting total TEP content in the mesocosms (Yet, see below section 3.2).

304 The relative uniformity and stability of TEP within the 15 m water column of both the
305 mesocosms and the lagoon waters reflects the homogeneity of the shallow lagoon system. The
306 variability between the three depths was statistically insignificant in many of the other
307 physical, chemical, and biological features of the mesocosms and the lagoon waters for
308 temperature, salinity, inorganic nutrients (N, P, Si), POC, PON, POP, DOC, Chl *a*, and
309 primary production and heterotrophic bacterial production (Berthelot et al., 2015; Van
310 Wambeke et al., This issue; Bonnet et al., This issue-b; Bonnet et al., This issue-a). In contrast
311 to some marine systems where TEP concentrations were correlated with the vertical
312 distribution of Chl *a* or POC (Passow, 2002; Engel, 2004; Ortega-Retuerta et al., 2009; Bar-
313 Zeev et al., 2009; Bar-Zeev et al., 2011), the results we obtained here showed no correlation



314 to the vertical (i.e. depth related) autotrophic signatures. Moreover, the similar TEP
315 concentrations at 1, 6, and 15 m do not support a sub-surface maxima in TEP concentrations,
316 stimulated by abiotic aggregation, at the sea-surface top layer as has been reported at 1 m
317 depth in different oceanic areas (Wurl et al., 2011). Abiotic processes of formation and
318 breakdown can be influential yet here we do not see a depth-correlated specific abiotic driver
319 and TEP were evenly distributed within the 15 m water column for all mesocosms (Fig. S1).

320 **3.2 DIP availability, APA, and TEP content.**

321 The average TEP concentrations we measured in the New Caledonian waters are
322 comparable to TEP concentrations reported from other marine environments such as the
323 eastern temperate-subarctic North Atlantic (Engel, 2004), the Ross Sea (Hong et al., 1997),
324 western Mediterranean – Gulf of Cadiz and the Straits of Gibraltar (García et al., 2002; Prieto
325 et al., 2006), the Gulf of Aqaba (northern Red Sea), (Bar-Zeev et al., 2009), in the northern
326 Adriatic Sea (Radić et al., 2005), and in the New Caledonia lagoon (Mari et al., 2007;
327 Rochelle-Newall et al., 2008).

328 While prediction as to the expected TEP concentrations with trophic or productive
329 status is difficult (Beauvais et al., 2003), decreasing availability of dissolved nutrients such as
330 nitrate and phosphate have been correlated with enriched TEP concentrations in both cultured
331 phytoplankton and natural marine systems (Engel et al., 2002; Brussaard et al., 2005; Urbani
332 et al., 2005; Bar-Zeev et al., 2011). In P-limited systems, low Chl *a* concentrations often
333 reflect the nutrient-stressed phytoplankton. As long as light and CO₂ are available, limitation
334 of essential nutrients results in an uncoupling between carbon fixation and growth during
335 which the excess photosynthate can be used to produce carbon-rich compounds including
336 TEP (Berman-Frank and Dubinsky, 1999; Mari et al., 2001; Rochelle-Newall et al., 2008).
337 Moreover, as DIP-availability declines, cells activate P-acquisition pathways and enzymes
338 such as APA to access P from other sources. Thus, and based on previous data (Bar-Zeev et
339 al., 2011), we hypothesized that TEP content would be negatively correlated with autotrophic
340 biomass (Chl *a*) and PP and positively correlated with APA.

341 Mesocosm fertilization on the evening of day 4 enriched the system with ten-fold
342 higher DIP concentrations that were available for microbial utilization throughout the
343 following 8 – 10 days (Berthelot et al., 2015; Van Wambeke et al., This issue; Leblanc et al.,
344 This issue; Bonnet et al., This issue-b). Thus, when DIP concentrations were relatively
345 sufficient during P1, no statistically significant relationship was observed between TEP and



346 POP, DIP, T_{DIP} , Chl *a*, or PP (Table S2). This situation changed with the declining availability
347 of DIP and the shift in the response of the system during P2 from day 15 to 23. During P2
348 high TEP concentrations were associated with decreasing DIP for each of the mesocosms with
349 an overall negative correlation ($R^2 = 0.23$, $n = 23$, $p = 0.02$), (Fig. 3a). A similar negative
350 trend was obtained between TEP and the turnover time of DIP (T_{DIP}) which can indicate DIP
351 limitation ($R^2=0.28$ $n= 26$, $p= 0.006$), (Fig. 3b).

352 In the South West Pacific, the critical DIP turnover time (T_{DIP}) required for single
353 filaments of *Trichodesmium* to grow is 2 d (Moutin et al., 2005). Here T_{DIP} values lower than
354 1 d, indicative of a strong DIP deficiency, were reached on day 14 in M1, day 19 for M2, and
355 on day 21 for M3 with the average T_{DIP} values during P2 significantly different in each
356 mesocosm, T_{DIP} of 0.5, 1.8, 3.9 d for M1, M2, M3, respectively (Berthelot et al., 2015). The
357 deficiency in DIP was reflected in the subsequent APA which increased rapidly in both M1
358 and M2 from day 18 (average for M1 and M2 during P2 $\sim 8 \pm 6$ nmol MUF l⁻¹ h⁻¹) and after
359 day 21 in M3 illustrating a biological response of the microbial community to P stress (Van
360 Wambeke et al., This issue). We did not specifically measure TEP production by autotrophic
361 or heterotrophic plankton. Yet, the significant (although indirect relationship) negative
362 correlation of TEP with DIP concentrations and T_{DIP} (Fig. 3a-b) suggests that microbial
363 responses to decreased DIP availability resulted from either 1) an increase in TEP synthesis
364 through higher polysaccharide production rather than biomass which requires higher nutrients
365 (Berman-Frank and Dubinsky 1999, (Wood and Van Valen, 1990), or 2) nutrient limitation
366 inducing greater breakdown of biomass and POM (maybe via programmed cell death) and
367 subsequent abiotic formation of TEP. We obtained a significant semi-logarithmic relationship
368 between TEP and APA ($R^2 = 0.33$ $n= 25$, $p = 0.002$), (Fig. 3c) which implies active TEP
369 formation when DIP concentrations are reduced and APA increases until a saturating point
370 whereby any further increases in APA do not appear to impact TEP concentrations (Fig. 3c).
371 This relationship may not always be valid as APA in the lagoon waters was consistently
372 higher at 1 m than APA measured at 6 and 12 m depths (Van Wambeke et al., This issue), yet
373 TEP concentrations were uniform at all depths (Fig. S1).

374 3.3 TEP and carbon pools

375 The size range of TEP spans a range of particles from 0.45 to 300 μm (Alldredge et al.,
376 1993; Bar-Zeev et al., 2015). TEP precursors (0.05 to 0.45 μm size) are formed and broken
377 down in the DOC pool and thus essentially “TEP establish a bridge between DOM (including



378 DOC) and the POM pool (Engel, 2004). Our data shows a generally stable contribution of
379 TEP to the TOC pool. Excluding day 5, where TEP-C comprised $56.5 \pm 8\%$ of TOC, the %
380 TEP-C was $28.9 \pm 9.3\%$ and $27.0 \pm 7.2\%$ of the TOC in all mesocosms and in the lagoon
381 waters, respectively (Fig. 4a-b).

382 TEP concentrations can be directly and positively correlated with POC (Engel, 2004)
383 and with DOC (Ortega-Retuerta et al., 2009). Yet, TEP concentrations can also be negatively
384 related to POC indicative of low TEP production when POC concentrations are high (Bar-
385 Zeev et al., 2011). In the mesocosms, a significant positive correlation between TEP
386 concentrations and TOC was obtained for all three mesocosms only during P2 ($R^2 = 0.75$,
387 0.73, 0.58 and $p < 0.05$ for M1, M2, M3 respectively), (Fig. 4c, Table S2). This period
388 coincided with the largest gain in total autotrophic and heterotrophic biomass and elevated N_2
389 fixation, PP, and BP rates (Berthelot et al., 2015; Van Wambeke et al., This issue; Bonnet et
390 al., This issue-a).

391 Although TEP was significantly and positively correlated with TOC in the mesocosms
392 during P2, this was not the case with either POC or DOC in any mesocosm for either P1 or P2
393 (Table 1). The absence of any significant correlation between TEP and POC was surprising as
394 TEP are part of the POC pool comprising 40 – 60% of the particulate combined carbohydrates
395 in POC (Engel, 2004; Engel et al., 2012). Furthermore, we did not obtain any significant
396 correlations of TEP and specific components of the dissolved organic matter such as
397 fluorescent dissolved organic matter (FDOM) or chromophoric dissolved organic matter
398 (CDOM) that was coupled to the dynamics of N_2 fixation in the mesocosms (Tedetti et al.,
399 This issue). The lack of significant correlation could partially reflect methodological issues. In
400 this experiment [and operationally according to published protocol (Passow and Alldredge
401 (1995)] TEP was measured on $0.45 \mu\text{m}$ filters – so that Alcian Blue stained particles included
402 particles $> 0.45 \mu\text{m}$ while POC was measured on GF/F (nominal pore size $0.7 \mu\text{m}$). DOC is
403 typically considered for the $< 0.45 \mu\text{m}$ fraction (Thurman, 1985), although here no direct
404 measurements of DOC were made and DOC was obtained by subtracting POC from TOC.
405 Thus, DOC actually covered the $< 0.7 \mu\text{m}$ fraction. Our methodology therefore precluded
406 determination of the smaller TEP precursors that would contribute to the DOC and colloidal
407 pools (Villacorte et al., 2015). As such we probably overestimated TEP relative to POC and at
408 the same time underestimated TEP's contribution to the DOC pool (Bar-Zeev et al., 2009).
409 The lacking correspondence between TEP concentrations and the pools of POC and DOC
410 may also result from the uncoupling between formation and breakdown processes. Abiotic



411 processes, will modify relationships obtained between biotic TEP production and recycling
412 (Wurl et al., 2011). Thus, it is feasible that especially during P1 abiotic factors predominated
413 breaking down larger TEP particles into smaller TEP precursors that would be mobilized to
414 the DOC pool and would thus maintain a relatively stable TEP pool although we observed a
415 positive increase in TEP with increased blooms of DDAs (see below section 3.4.1).

416

417 **3.4 Production and utilization of TEP by primary and bacterial populations**

418 Typically TEP are formed by diverse algal and bacterial species (Mari and Burd 1998)
419 yet are utilized mostly by bacteria and grazers as a rich C source (Engel and Passow, 2001;
420 Azam and Malfatti, 2007; Bar-Zeev et al., 2015). Throughout this experiment (P1 and P2
421 stages) TEP was not significantly correlated to parameters related to autotrophic production
422 such as total Chl *a*, PP, non-diazotrophic diatom or cyanobacterial abundance, or the growth
423 and mortality rates of these populations (Table S2). Furthermore, during P1, no significant
424 relationship between TEP and BA (total or specific for high and low nucleic acid bacteria-
425 HNA or LNA respectively), BP, or division rates was noted in any of the mesocosms (Table
426 S2).

427 This changed during P2 when TEP was positively correlated to the increasing BP for all
428 three mesocosms (Pearson's correlation coefficient $R^2 = 0.63, 0.66, 0.69$ for M1, M2, and M3
429 respectively, $p < 0.05$), (Fig. 5). During P2, TEP was also strongly and positively correlated to
430 TOC, which significantly increased over this time period (Fig. 4c) due to the high production
431 rates of both photosynthetic and heterotrophic bacterial populations. However, although BP
432 and PP were positively associated during P2 (log-log transformation, Fig. 5 in Van Wambeke
433 et al. this issue), we found no direct correlation between TEP and PP for either linear (Table
434 S2) or log-transformed regression (not shown). This coupling between PP and BP, while a
435 concurrent association between TEP and BP occurred during P2, indicates TEP may have been
436 utilized by bacteria as a carbon source (Azam, 1998; Ziervogel et al., 2014) or provided a
437 suitable niche for aggregation and proliferation of heterotrophic bacteria.

438 **3.4.1 TEP and diazotrophic populations**

439 Overall N_2 fixation rates were not significantly correlated with TEP concentrations at
440 any time in the experiment (Table S2). Neither could we discern any direct evidence of TEP
441 providing a carbon source for heterotrophic diazotrophs as was found previously in the Gulf
442 of Aqaba where these organisms contributed greatly to the N_2 fixation rates (Rahav et al.,



443 2015). Indeed, no relationship was found between TEP concentrations and the abundance or
444 growth rates of the heterotrophic diazotrophs γ -24774A11 (Moisander et al., 2014). Although
445 these organisms were present throughout the experiment, and increased ~4 fold from day 9 to
446 15 especially in M3, they contributed only a small fraction to the total diazotrophic biomass
447 and N_2 fixation rates (Turk-Kubo et al., 2015).

448 Yet, discerning individual diazotroph populations revealed some species-specific
449 correspondence to TEP at certain periods during the experiment. For example, throughout the
450 experiment, net growth rates (i.e., based on differences of *nifH* copies L^{-1} from day to day) of
451 the DDA *Richelia* (Het-1) associated with *Rhizosolenia* (Turk-Kubo et al., 2015) temporally
452 paralleled TEP concentrations in all mesocosms (Fig. 6a-c, Fig. 6e-f). During both P1 and P2
453 TEP concentrations were positively correlated with the net growth rates of Het-1 ($R^2=0.6$
454 $P=0.0001$, $n=19$ for all mesocosms (Fig. 6d). Although the DDAs dominated the diazotroph
455 community during P1 (primarily Het-1), their overall contribution to diatom biomass in the
456 mesocosm was low with only 2-8% of all diatom biomass (Leblanc et al., this issue). We did
457 not observe an overall relationship between TEP and total diatom biomass throughout
458 VAHINE although diatoms are well known for their TEP production especially when
459 nutrients are limiting and growth rates decline (Urbani et al., 2005; Fukao et al., 2010). Thus,
460 the positive association between TEP and the growth rates of Het-1 and not of the other
461 DDAs Het-2 and Het-3 is intriguing.

462 TEP was also associated with the growth rates of the unicellular UCYN-C diazotrophs
463 that bloomed during P2 and dominated the N_2 fixation rates or this period (Turk-Kubo et al.,
464 2015; Berthelot et al., 2015). During P2, UCYN-C net growth rates were positively correlated
465 with increasing TEP concentrations ($R^2=0.65, 0.83, 0.88$ for M1, M2, M3 respectively, $p <$
466 0.05). Furthermore, UCYN-C formed large aggregates (100-500 μm) embedded in an organic
467 matrix possibly also comprised of TEP (Fig. 6g-h) and were predominantly responsible for
468 the enhanced export production ($22.4 \pm 5\%$ of exported POC), (Knapp et al., This issue;
469 Bonnet et al., This issue-a). High TEP content was obtained from sediment traps on days 15
470 and 16 (Fig. S1), corresponding to the height of the UCYN-C bloom in the mesocosms (Turk-
471 Kubo et al., 2015) and substantiating the role of TEP in facilitating export flux in the New
472 Caledonia lagoon (Mari et al., 2007).

473 The diazotroph *Trichodesmium*, that can account for huge surface blooms in the New
474 Caledonia lagoons (Rodier and Le Borgne, 2008; Rodier and Le Borgne, 2010), did not bloom
475 or accumulate within the VAHINE mesocosms. Yet, on day 23 a dense surface accumulation



476 was sighted on the surface of the lagoon waters (Spungin et al., This issue). Frequent
477 sampling (every 2-4 h) over the subsequent two days yielded extremely high TEP
478 concentrations ($> 800 \mu\text{g GX L}^{-1}$) from this rapidly declining biomass (Spungin et al., This
479 issue) corresponding to previous work demonstrating high TEP concentrations in
480 *Trichodesmium* from the New Caledonian lagoon that are undergoing autocatalytic
481 programmed cell death (PCD), (Berman-Frank et al., 2004; Berman-Frank et al., 2007; Bar-
482 Zeev et al., 2013). We showed that nutrient stressed, PCD-induced *Trichodesmium* diverts
483 available carbon from growth processes to produce large amounts of TEP (Berman-Frank and
484 Dubinsky, 1999; Berman-Frank et al., 2007). The TEP produced combines with the decaying
485 biomass to form large particles and aggregates that sink downwards (Bar-Zeev et al., 2013).
486 Here, we could not quantify the flux of matter obtained after this ephemeral bloom crashed.
487 Yet, it is reasonable to assume that the high TEP content and the $> 90\%$ decline in biomass
488 over a 24 h period resulted in a large downward flux of TEP-cellular debris aggregates as we
489 had observed previously under laboratory experiments (Berman-Frank et al., 2007; Bar-Zeev
490 et al., 2013).

491

492 **4 Conclusions**

493 Although physically separated from the surrounding lagoon, TEP formation and
494 breakdown was difficult to tease out in the VAHINE mesocosms where abiotic drivers
495 (turbulence, shear forces, chemical coagulation) and biotic processes (algal and bacterial
496 production and utilization) maintained an apparently constant pool of TEP within the TOC.
497 Total TEP content was generally stable throughout the experimental period of 23 days and
498 comprised $\sim 28\%$ of the TOC in the mesocosms and lagoon with uniform distribution in the
499 three sampled depths of the 15 m deep-water column.

500 TEP concentrations appeared to be impacted indirectly via changes in DIP availability
501 as it was biologically consumed in the mesocosms after fertilization. Thus, declining P
502 availability (low DIP, rapid T_{DIP} , and increased APA) was associated with higher TEP content
503 in all mesocosms. TEP concentrations were also positively associated with net growth rates of
504 two important diazotrophic groups: the DDA *Richelia-Rhizosolenia* (Fig. 6e-f), during P1 and
505 P2 (excluding days 21-23); and UCYN-C diazotrophs which bloomed during P2. High TEP
506 content in the sediment traps during the UCYN-C bloom indicates that TEP may have been
507 part of the organic matrix associated with the large aggregates of UCYN-C that were exported
508 to the sediment traps (Fig. 6g-h).



509 TEP may have also provided bacteria with a rich organic carbon source especially
510 during P2 when higher BP (stimulated by the higher PP) was positively correlated higher TEP
511 concentrations. High production of TEP also occurred in the lagoon water outside the
512 mesocosms on day 23 during the decline of a short-lived dense surface bloom of the
513 diazotrophic *Trichodesmium* (Spungin et al., This issue) . Our results emphasize the
514 complexities of the natural system and suggest that to understand the role of compounds such
515 as TEP, and their contribution to the DOC and POC pools, a wider perspective and
516 methodologies be undertaken to examine and characterize the different components of marine
517 gels (not only carbohydrate-based), (Verdugo, 2012; Bar-Zeev et al., 2015)

518

519 **Author contributions**

520 IBF conceived and designed the investigation of TEP dynamics within the VAHINE project.
521 TM, FVW, IBF, DS, and ER participated in the experiment and performed analyses of
522 samples and data, KTK analysed diazotrophic populations. IBF and DS wrote the manuscript
523 with contributions from all co-authors.

524

525 **Acknowledgements**

526 Many thanks to Sophie Bonnet who created, designed, and successfully executed the
527 VAHINE project .The participation of IBF, DS, and ER in the VAHINE experiment was
528 supported by the German-Israeli Research Foundation (GIF), project number 1133-13.8/2011
529 to IBF and through a collaborative grant to IBF and SB from MOST Israel and the High
530 Council for Science and Technology (HCST)-France. Funding for this research was provided
531 by the Agence Nationale de la Recherche (ANR starting grant VAHINE ANR-13-JS06-0002),
532 INSU-LEFE-CYBER program, GOPS, IRD and M.I.O The authors thank the captain and
533 crew of the R/V Alis; the SEOH divers service from the IRD research center of Noumea (E.
534 Folcher, B. Bourgeois and A. Renaud) and from the Observatoire Océanologique de
535 Villefranche-sur-mer (OOV, J.M. Grisoni), the technical service and support of the IRD
536 research center of Noumea. Thanks also to C. Guieu, F. Louis and J.M. Grisoni from OOV for
537 mesocosm design and deployment advice. Special thanks to H. Berthelot and all other
538 participants and PIs of the project for the joint efforts and for making their data available for



539 further analyses. This work is in partial fulfillment of the requirements for a PhD thesis for D.
540 Spungin at Bar Ilan University.

541

542

543 References

544

545 Alldredge, A. L., Passow, U., and Logan, B. E.: The abundance and significance of a class of
546 large, transparent organic particles in the ocean., *Deep Sea Research*, 40, 1131-1140, 1993.

547 Aminot, A., and K erouel, R.: Dosage automatique des nutriments dans les eaux marines:
548 m ethodes en flux continu, Editions Quae, 2007.

549 Azam, F.: Microbial control of oceanic carbon flux: The plot thickens., *Science*, 280, 694-
550 696, 1998.

551 Azam, F., and Malfatti, F.: Microbial structuring of marine ecosystems, *Nature Reviews*
552 *Microbiology*, 5, 782-791, 2007.

553 Azetsu-Scott, K., and Passow, U.: Ascending marine particles: significance of transparent
554 exopolymer particles (TEP) in the upper ocean., *Limnol. & Oceanogr*, 49, 741-748, 2004.

555 Bar-Zeev, E., Berman-Frank, I., Liberman, B., Rahav, E., Passow, U., and Berman, T.:
556 Transparent exopolymer particles: Potential agents for organic fouling and biofilm formation
557 in desalination and water treatment plants, *Desalination and Water Treatment*, 3, 136-142,
558 2009.

559 Bar-Zeev, E., Berman, T., Rahav, E., Dishon, G., Herut, B., Kress, N., and Berman-Frank, I.:
560 Transparent exopolymer particle (TEP) dynamics in the eastern Mediterranean Sea, *Marine*
561 *Ecology-Progress Series*, 431, 107-118, 10.3354/meps09110, 2011.

562 Bar-Zeev, E., Avishay, I., Bidle, K. D., and Berman-Frank, I.: Programmed cell death in the
563 marine cyanobacterium *Trichodesmium* mediates carbon and nitrogen export, *The ISME*
564 *journal*, 7, 2340-2348, 2013.

565 Bar-Zeev, E., Passow, U., Romero-Vargas Castrill on, S., and Elimelech, M.: Transparent
566 exopolymer particles: from aquatic environments and engineered systems to membrane
567 biofouling, *Environmental science & technology*, 49, 691-707, 2015.

568 Beauvais, S., Pedrotti, M. L., Villa, E., and Lemee, R.: Transparent exopolymer particle
569 (TEP) dynamics in relation to trophic and hydrological conditions in the NW Mediterranean
570 Sea, *Marine Ecology-Progress Series*, 262, 97-109, 2003.

571 Benavides, M., Moisander, P., Berthelot, H., Dittmar T, rosso O, and Bonnet S: Mesopelagic
572 heterotrophic N₂ fixation related to organic matter composition in the Solomon and Bismarck
573 Seas (Southwest Pacific), *PLoS ONE*, in press.

574 Berman-Frank, I., and Dubinsky, Z.: Balanced growth in aquatic plants: Myth or reality?
575 Phytoplankton use the imbalance between carbon assimilation and biomass production to their
576 strategic advantage, *Bioscience*, 49, 29-37, 1999.



- 577 Berman-Frank, I., Bidle, K., Haramaty, L., and Falkowski, P.: The demise of the marine
578 cyanobacterium, *Trichodesmium* spp., via an autocatalyzed cell death pathway, *Limnol.*
579 *Oceanogr.*, 49, 997-1005, 2004.
- 580 Berman-Frank, I., Rosenberg, G., Levitan, O., Haramaty, L., and Mari, X.: Coupling between
581 autocatalytic cell death and transparent exopolymeric particle production in the marine
582 cyanobacterium *Trichodesmium*, *Environmental microbiology*, 9, 1415-1422, 2007.
- 583 Berthelot, H., Moutin, T., L'Helguen, S., Leblanc, K., Hélias, S., Grosso, O., Leblond, N.,
584 Charrière, B., and Bonnet, S.: Dinitrogen fixation and dissolved organic nitrogen fueled
585 primary production and particulate export during the VAHINE mesocosm experiment (New
586 Caledonia lagoon), *Biogeosciences*, 12, 4099-4112, 10.5194/bg-12-4099-2015, 2015.
- 587 Biegala, I. C., and Raimbault, P.: High abundance of diazotrophic picocyanobacteria (< 3 μm)
588 in a Southwest Pacific coral lagoon, *Aquatic microbial ecology*, 51, 45-53, 2008.
- 589 Bonnet, S., Berthelot, H., Turk-Kubo, K., Fawcett, S., Rahav, E., Berman-Frank, I., and
590 l'Helguen, S.: Dynamics of N_2 fixation and fate of diazotroph-derived nitrogen during the
591 VAHINE mesocosm experiment (New Caledonia), This issue-a.
- 592 Bonnet, S., Helias, S., Rodier, M., Moutin, T., Grisoni, J. M., Louis, F., Folcher, E.,
593 Bourgeois, B., Boré, J. M., and Renaud, A.: Introduction to the project VAHINE: VAriability
594 of vertical and trophic transfer of diazotroph derived N in the South West Pacific, This issue-
595 b.
- 596 Brussaard, C., Mari, X., Van Bleijswijk, J., and Veldhuis, M.: A mesocosm study of
597 *Phaeocystis globosa* (Prymnesiophyceae) population dynamics: II. Significance for the
598 microbial community, *Harmful algae*, 4, 875-893, 2005.
- 599 Capone, D. G.: Marine nitrogen fixation: what's the fuss?, *Curr. Opin. Microbiol.*, 4, 341-348,
600 2001.
- 601 Duhamel, S., Zeman, F., and Moutin, T.: A dual-labeling method for the simultaneous
602 measurement of dissolved inorganic carbon and phosphate uptake by marine planktonic
603 species, *Limnology and Oceanography-Methods*, 4, 416-425, 2006.
- 604 Dupouy, C., Neveux, J., Subramaniam, A., Mulholland, M. R., Montoya, J. P., Campbell, L.,
605 Capone, D. G., and Carpenter, E. J.: Satellite captures *Trichodesmium* blooms in the
606 SouthWestern Tropical Pacific., *EOS, Trans American Geophysical Union.*, 81, 13-16, 2000.
- 607 Engel, A.: The role of transparent exopolymer particles (TEP) in the increase in apparent
608 particle stickiness (α) during the decline of a diatom bloom, *Journal of Plankton Research*, 22,
609 485-497, 2000.
- 610 Engel, A., and Passow, U.: Carbon and nitrogen content of transparent exopolymer particles
611 (TEP) in relation to their Alcian Blue adsorption, *Marine Ecology Progress Series*, 219, 1-10,
612 2001.
- 613 Engel, A., Goldthwait, S., Passow, U., and Alldredge, A.: Temporal decoupling of carbon and
614 nitrogen dynamics in a mesocosm diatom bloom, *Limnology and Oceanography*, 47, 3, 753-
615 761, 2002.
- 616 Engel, A.: Distribution of transparent exopolymer particles (TEP) in the northeast Atlantic
617 Ocean and their potential significance for aggregation processes, *Deep-Sea Research Part I-*
618 *Oceanographic Research Papers*, 51, 83-92, 2004.



- 619 Engel, A., Harlay, J., Piontek, J., and Chou, L.: Contribution of combined carbohydrates to
620 dissolved and particulate organic carbon after the spring bloom in the northern Bay of Biscay
621 (North-Eastern Atlantic Ocean), *Continental shelf research*, 45, 42-53, 2012.
- 622 Eppley, R. W., and Peterson, B. J.: Particulate organic-matter flux and planktonic new
623 production in the deep ocean, *Nature*, 282, 677-680, 10.1038/282677a0, 1979.
- 624 Falkowski, P. G.: Evolution of the nitrogen cycle and its influence on the biological
625 sequestration of CO₂ in the ocean, *Nature*, 387, 272-275, 1997.
- 626 Fukao, T., Kimoto, K., and Kotani, Y.: Production of transparent exopolymer particles by four
627 diatom species, *Fisheries science*, 76, 755-760, 2010.
- 628 García, C., Prieto, L., Vargas, M., Echevarría, F., Garcia-Lafuente, J., Ruiz, J., and Rubin, J.:
629 Hydrodynamics and the spatial distribution of plankton and TEP in the Gulf of Cadiz (SW
630 Iberian Peninsula), *Journal of Plankton Research*, 24, 817-833, 2002.
- 631 Garcia, N., Raimbault, P., and Sandroni, V.: Seasonal nitrogen fixation and primary
632 production in the Southwest Pacific: nanoplankton diazotrophy and transfer of nitrogen to
633 picoplankton organisms, *Marine Ecology-Progress Series*, 343, 25-33, 10.3354/meps06882,
634 2007.
- 635 Grossart, H. P., Simon, M., and Logan, B. E.: Formation of macroscopic organic aggregates
636 (lake snow) in a large lake: The significance of transparent exopolymer particles, plankton,
637 and zooplankton, *Limnology and Oceanography*, 42, 1651-1659, 1997.
- 638 Hong, Y., Smith, W. O., and White, A. M.: Studies on transparent exopolymer particles (TEP)
639 produced in the ross sea (antarctica) and by *Phaeocystis antarctica* (prymnesiophyceae),
640 *Journal of Phycology*, 33, 368-376, 1997.
- 641 Hoppe, H. G.: Significance of exoenzymatic activities in the ecology of brackish water:
642 measurements by means of methylumbelliferyl-substrates. , *Marine Ecology Progress Series*,
643 11, 299-308, 1983.
- 644 Kirchman, D.: Leucine incorporation as a measure of biomass production by heterotrophic
645 bacteria, *Handbook of methods in aquatic microbial ecology*. Lewis, 509-512, 1993.
- 646 Knapp, A. N., Fawcett, S. E., Martinez-Garcia, A., Haug, G., Leblond, N., Moutin, T., and
647 Sophie., B.: Nitrogen isotopic evidence for a shift from nitrate- to diazotroph-fueled export
648 production in VAHINE mesocosm experiments, This issue.
- 649 Leblanc, K., Cornet, V., Caffin, M., Rodier, M., Desnues, A., Berthelot, H., Heliou, J., and
650 Bonnet, S.: Phytoplankton community structure in the VAHINE mesocosm experiment, This
651 issue.
- 652 Logan, B. E., Passow, U., Alldredge, A. L., Grossart, H.-P., and Simon, M.: Rapid formation
653 and sedimentation of large aggregates is predictable from coagulation rates (half-lives) of
654 transparent exopolymer particles (TEP), *Deep Sea Research Part II: Topical Studies in
655 Oceanography*, 42, 203-214, 1995.
- 656 Mari, X., Beauvais, S., Lemée, R., and Pedrotti, M. L.: Non-Redfield C: N ratio of transparent
657 exopolymeric particles in the northwestern Mediterranean Sea, *Limnology and
658 Oceanography*, 46, 1831-1836, 2001.
- 659 Mari, X., Kerros, M. E., and Weinbauer, M. G.: Virus attachment to transparent exopolymeric
660 particles along trophic gradients in the southwestern lagoon of New Caledonia, *Applied and
661 Environmental Microbiology*, 73, 5245-5252, 10.1128/aem.00762-07, 2007.



- 662 Moisaner, P. H., Serros, T., Paerl, R. W., Beinart, R. A., and Zehr, J. P.:
663 Gammaproteobacterial diazotrophs and *nifH* gene expression in surface waters of the South
664 Pacific Ocean, *The ISME journal*, 8, 1962-1973, 2014.
- 665 Moutin, T., Thingstad, T. F., Van Wambeke, F., Marie, D., Slawyk, G., Raimbault, P., and
666 Claustre, H.: Does competition for nanomolar phosphate supply explain the predominance of
667 the cyanobacterium *Synechococcus*?, *Limnology and Oceanography*, 47, 1562-1567, 2002.
- 668 Moutin, T., Van Den Broeck, N., Beker, B., Dupouy, C., Rimmelin, P., and Le Bouteiller, A.:
669 Phosphate availability controls *Trichodesmium* spp. biomass in the SW Pacific Ocean, *Marine
670 Ecology-Progress Series*, 297, 15-21, 2005.
- 671 Mulholland, M. R., and Capone, D. G.: The nitrogen physiology of the marine N₂-fixing
672 cyanobacteria *Trichodesmium* spp, *Trends in plant science*, 5, 148-153, 2000.
- 673 Ortega-Retuerta, E., Reche, I., Pulido-Villena, E., Agustí, S., and Duarte, C. M.: Uncoupled
674 distributions of transparent exopolymer particles (TEP) and dissolved carbohydrates in the
675 Southern Ocean, *Marine chemistry*, 115, 59-65, 2009.
- 676 Passow, U., and Alldredge, A. L.: A dye binding assay for the spectrophotometric
677 measurement of transparent exopolymer particles (TEP), *Limnol. & Oceanogr*, 40, 1326-
678 1335, 1995.
- 679 Passow, U.: Transparent exopolymer particles (TEP) in aquatic environments, *Progress in
680 Oceanography*, 55, 287-333, 2002.
- 681 Postgate, J. R., and Eady, R. R.: The evolution of biological nitrogen fixation, in: *Nitrogen
682 Fixation: One Hundred Years After*, edited by: Bothe, H., DeBruijn, F. J., Newton, W.E,
683 Gustav Fischer, Stuttgart, 31-40., 1988.
- 684 Prieto, L., Navarro, G., Cozar, A., Echevarria, F., and García, C. M.: Distribution of TEP in
685 the euphotic and upper mesopelagic zones of the southern Iberian coasts, *Deep Sea Research
686 Part II: Topical Studies in Oceanography*, 53, 1314-1328, 2006.
- 687 Radić, T., Degobbis, D., Fuks, D., Radić, J., and Đakovac, T.: Seasonal cycle of transparent
688 exopolymer particles' formation in the northern Adriatic during years with (2000) and without
689 mucilage events (1999), *Fresenius environmental bulletin*, 14, 224-230, 2005.
- 690 Rahav, E., Bar-Zeev, E., Ohayion, S., Elifantz, H., Belkin, N., Herut, B., Mulholland, M. R.,
691 and Berman-Frank, I. R.: Dinitrogen fixation in aphotic oxygenated marine environments,
692 *Frontiers in Microbiology*, 4, 10.3389/fmicb.2013.00227, 2013.
- 693 Rahav, E., Herut, B., Mulholland, M. R., Belkin, N., Elifantz, H., and Berman-Frank, I.:
694 Heterotrophic and autotrophic contribution to dinitrogen fixation in the Gulf of Aqaba,
695 *Marine Ecology Progress Series*, 522, 67-77, 2015.
- 696 Rochelle-Newall, E., Torretón, J.-P., Mari, X., and Pringault, O.: Phytoplankton-
697 bacterioplankton coupling in a subtropical South Pacific coral reef lagoon, *Aquatic Microbial
698 Ecology*, 50, 221, 2008.
- 699 Rodier, M., and Le Borgne, R.: Population dynamics and environmental conditions affecting
700 *Trichodesmium* spp. (filamentous cyanobacteria) blooms in the south-west lagoon of New
701 Caledonia, *Journal of Experimental Marine Biology and Ecology*, 358, 20-32,
702 10.1016/j.jembe.2008.01.016, 2008.



- 703 Rodier, M., and Le Borgne, R.: Population and trophic dynamics of *Trichodesmium thiebautii*
 704 in the SE lagoon of New Caledonia. Comparison with *T. erythraeum* in the SW lagoon,
 705 Marine Pollution Bulletin, 61(7-12), 349-359, 10.1016/j.marpolbul.2010.06.018, 2010.
- 706 Smith, D. C., and Azam, F.: A simple, economic method for measuring bacterial protein
 707 synthesis rates in seawater using ³H-leucine Mar. Microb. Food Webs 6, 107-114, 1992.
- 708 Spungin, D., Pfreundt, U., Berthelot, H., Bonnet, S., Al-Roumi, D., Natale, F., Hess, W. R.,
 709 Bidle, K. D., and Berman-Frank, I.: Mechanisms of *Trichodesmium* bloom demise within the
 710 New Caledonia Lagoon, This issue.
- 711 Stam, H., Stouthamer, A. H., and van Verseveld, H. W.: Hydrogen metabolism and energy
 712 costs of nitrogen fixation, FEMS Microbiology Reviews, 46, 73-92, 1987.
- 713 Stoderegger, K. E., and Herndl, G. J.: Production of exopolymer particles by marine
 714 bacterioplankton under contrasting turbulence conditions, Marine Ecology Progress Series,
 715 189, 9-16, 1999.
- 716 Tedetti, M., Marie, L., Röttgers, R., Rodier, M., Van Wambeke, F., Helias, S., Caffin, M.,
 717 Cornet-Barthaux, V., and Dupouy, C.: Evolution of dissolved and particulate chromophoric
 718 materials during the VAHINE mesocosm experiment in the New Caledonian coral lagoon
 719 (South West Pacific), This issue.
- 720 Thurman, E.: Organic Geochemistry of Natural Waters, Martinus Nijhoff/Dr W. Junk
 721 Publishers, Dordrecht, 1985.
- 722 Turk-Kubo, K., Frank, I., Hogan, M., Desnues, A., Bonnet, S., and Zehr, J.: Diazotroph
 723 community succession during the VAHINE mesocosms experiment (New Caledonia Lagoon),
 724 Biogeosciences Discussions, 12, 2015.
- 725 Urbani, R., Magaletti, E., Sist, P., and Cicero, A. M.: Extracellular carbohydrates released by
 726 the marine diatoms *Cylindrotheca closterium*, *Thalassiosira pseudonana* and *Skeletonema*
 727 *costatum*: Effect of P-depletion and growth status, Science of the Total Environment, 353,
 728 300-306, 2005.
- 729 Van Wambeke, F., Pfreundt, U., Barani, A., Berthelot, H., Moutin, T., Rodier, M., Hess,
 730 W.R., and S, B.: Heterotrophic bacterial production and metabolic balance during the
 731 VAHINE mesocosm experiment in the New Caledonia lagoon, Biogeosciences Discussions,
 732 This issue.
- 733 Verdugo, P., and Santschi, P. H.: Polymer dynamics of DOC networks and gel formation in
 734 seawater, Deep Sea Research Part II: Topical Studies in Oceanography, 57, 1486-1493, 2010.
- 735 Verdugo, P.: Marine microgels, Annual review of marine science, 4, 375-400, 2012.
- 736 Villacorte, L. O., Ekowati, Y., Calix-Ponce, H. N., Schippers, J. C., Amy, G. L., and
 737 Kennedy, M. D.: Improved method for measuring transparent exopolymer particles (TEP) and
 738 their precursors in fresh and saline water, Water research, 70, 300-312, 2015.
- 739 Wood, A., and Van Valen, L.: Paradox lost? On the release of energy-rich compounds by
 740 phytoplankton, 1990.
- 741 Wurl, O., Miller, L., and Vagle, S.: Production and fate of transparent exopolymer particles in
 742 the ocean, Journal of Geophysical Research: Oceans (1978–2012), 116, 2011.
- 743 Zehr, J. P., and Kudela, R. M.: Nitrogen Cycle of the Open Ocean: From Genes to
 744 Ecosystems, in: Annual Review of Marine Science, Vol 3, Annual Review of Marine Science,
 745 197-225, 2011.



746 Zhou, J., Mopper, K., and Passow, U.: The role of surface-active carbohydrates in the
747 formation of transparent exopolymer particles by bubble adsorption of seawater, *Limnology*
748 and *Oceanography*, 43, 1860-1871, 1998.

749 Ziervogel, K., D'souza, N., Sweet, J., Yan, B., and Passow, U.: Natural oil slicks fuel surface
750 water microbial activities in the northern Gulf of Mexico, *Frontiers in microbiology*, 5, 2014.

751

752



753 **Figure legends**

754 **Figure 1.** Temporal changes in transparent exopolymeric particle (TEP) concentrations (μg
 755 GX L^{-1}) during the VAHINE mesocosm experiment. Data shown are from daily sampling of
 756 three depths (1, 6, 12 m) in each mesocosm. Data was analyzed according to the characterized
 757 phases of the experiment based on the diazotrophic communities that developed in the
 758 mesocosms (Turk-Kubo et al., 2015) and biogeochemical characteristics (Bonnet et al., This
 759 issue-a). **a.** Mesocosm 1 (M1) **b.** Mesocosm 2 (M2), **c.** Mesocosm 3 (M3), **d.** samples from
 760 the lagoon waters outside of the mesocosms (O). Phases: P0= days 2-4, P1= days 5-14, P2=
 761 days 15-23. Linear regressions (Pearson) of TEP for each of the phases are designated by a
 762 solid line, only when significant. Pearson correlations coefficients and significant values ($p <$
 763 0.05) are represented in bold in Table S1.

764 **Figure 2.** Total content of transparent exopolymeric particles (TEP) per mesocosm and in the
 765 lagoon waters surrounding the mesocosms. The average amount in $\text{g GX mesocosm}^{-1}$ for the
 766 two periods of the experiment after DIP fertilization was calculated from the total daily
 767 amount based on concentrations measured at three depths and integrated for the specific
 768 volume per mesocosm or for an equivalent volume of lagoon water. Averages are represented
 769 in boxplots as a function of two different phases: P1 = days 5-14 and P2 = days 15-23. Red
 770 (mesocosm 1 - M1), blue (mesocosm 2- M2), green (mesocosm - M3) and black (Outside
 771 lagoon O). Straight lines within the boxes mark the median. No significant differences were
 772 observed between the phases or between the three mesocosms and the outside lagoon
 773 (Kruskal-Wallis non-parametric analysis of variance; $p > 0.05$).

774 **Figure 3.** Relationships between the concentration of transparent exopolymeric particles
 775 (TEP), ($\mu\text{g GX L}^{-1}$) and **a.** dissolved inorganic phosphorus DIP ($\mu\text{mol L}^{-1}$), **b.** turnover time of
 776 $\text{DIP} - T_{\text{DIP}}$ (d) and **c.** alkaline phosphatase activity (APA), ($\text{nmol L}^{-1} \text{h}^{-1}$) in the three
 777 mesocosms (M1-red; M2-blue; M3-green) during phase 2 (days 15-23). For a and b Pearson
 778 linear regressions yielded an $R^2 = 0.54$, $n=23$ (TEP/DIP) and an $R^2=0.52$, $n=26$ (TEP/ T_{DIP}),
 779 and for c. Log-transformed ($\log(\text{TEP}) / \log(\text{APA})$) with R^2 0.68, $n=25$. All correlations were
 780 significant ($p < 0.05$). Error bars represent ± 1 standard deviation.

781 **Figure 4. a.** Temporal dynamics of TEP carbon concentrations (TEP-C, μM) in relationship
 782 to the average total organic carbon (TOC), ($\mu\text{g L}^{-1}$), (thin black line) in the mesocosms (M1-
 783 red dots, M2-blue dots, M3-green dots, and black dots- Outside waters (O). Black solid line
 784 designates TEP-C averaged for the three mesocosms (thick black line). TEP-C was measured



785 from 6 m depths and calculated according to Engel (2000). **b.** Temporal changes in the
786 percent of TEP-C from TOC (%) in mesocosms (green dots), and %TEP-C in the lagoon
787 waters (Out), (black dots). **c.** Relationship between TEP concentrations ($\mu\text{g GX L}^{-1}$) and TOC
788 ($\mu\text{mole L}^{-1}$), during phase 2 (days 15-23) for Mesocosm 1 (M1, red dots), Mesocosm 2 (M2,
789 blue dots), Mesocosm 3 (M3, green dots). Significant correlations were observed (Pearson)
790 for all mesocosms. $R^2 = 0.75$ - M1, 0.73 -M2, and 0.58 -M3 respectively, $n=7-8$, $p < 0.05$.
791 All statistics are detailed in Table S2. ($p=0.05$, $n=7-8$). Error bars represent ± 1 standard
792 deviation.

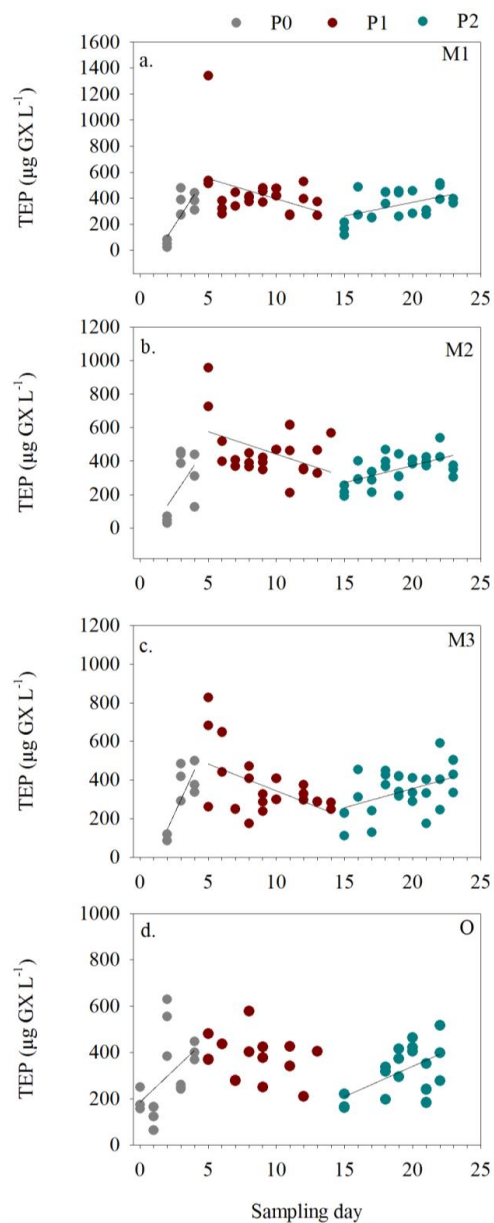
793 **Figure 5.** Relationship between heterotrophic bacterial production (BP), ($\text{ng C L}^{-1} \text{ h}^{-1}$) and
794 TEP concentrations ($\mu\text{g GX L}^{-1}$) during phase 2 (days 15-23) when BP increased following
795 the enhanced PP (Van Wambeke et al., This issue), for Mesocosm 1 (M1, red dots),
796 Mesocosm 2 (M2, blue dots), Mesocosm 3 (M3, green dots). Pearson's linear regressions
797 yielded $R^2 = 0.57$ for M1, 0.42 for M2, and 0.56 for M3 respectively. Significant correlations
798 were observed for all mesocosms and are detailed in Table S2. Error bars represent ± 1
799 standard deviation.

800 **Figure 6.** Temporal changes in TEP concentrations and Het-1 net growth rates (d^{-1}), (gray
801 triangles) for **a.** Mesocosm 1 (M1) **b.** Mesocosm 2 (M2), **c.** Mesocosm 3 (M3). TEP
802 concentrations were averaged from the three depths sampled per mesocosm (green circles).
803 Het-1 net growth rates were calculated based on changes of *nifH* copies L^{-1} (Turk-Kubo et al.,
804 2015) measured every other day. **d.** Relationship between TEP concentrations ($\mu\text{g GX L}^{-1}$)
805 and
806 Het-1 growth rate (d^{-1}) for all three mesocosms. Significant correlations were observed
807 (Pearson) from all mesocosms together. $R^2 = 0.60$, $p=0.0001$, $n=19$. Error bars represent ± 1
808 standard deviation. **e-f.** Epifluorescent microscopical images of the diatom-diazotroph
809 association *Richelia-Rhizosolenia* identified by Het-1 abundance. Images by V. Cornet-
810 Barthaux. **g-h.** the diazotroph UCYN-C which bloomed and formed large aggregates
811 (comprised also of TEP) that enhanced vertical flux and export production during P2. Images
812 by S. Bonnet.
813



814 **Figure 1**

815



837

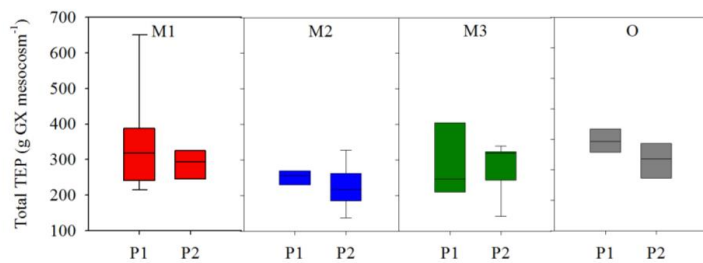
838

839



840 **Figure 2**

841



847

848

849

850

851

852

853

854

855

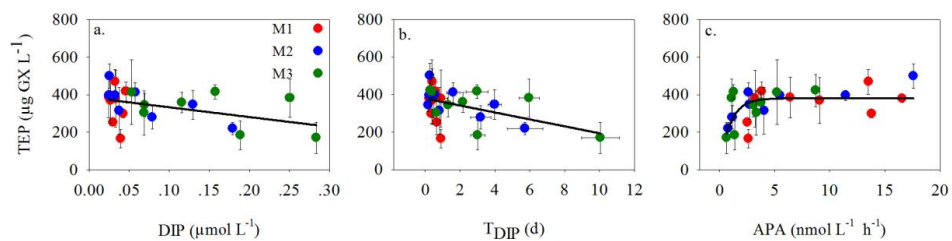
856



857 **Figure 3**

858

859



860

861

862

863

864



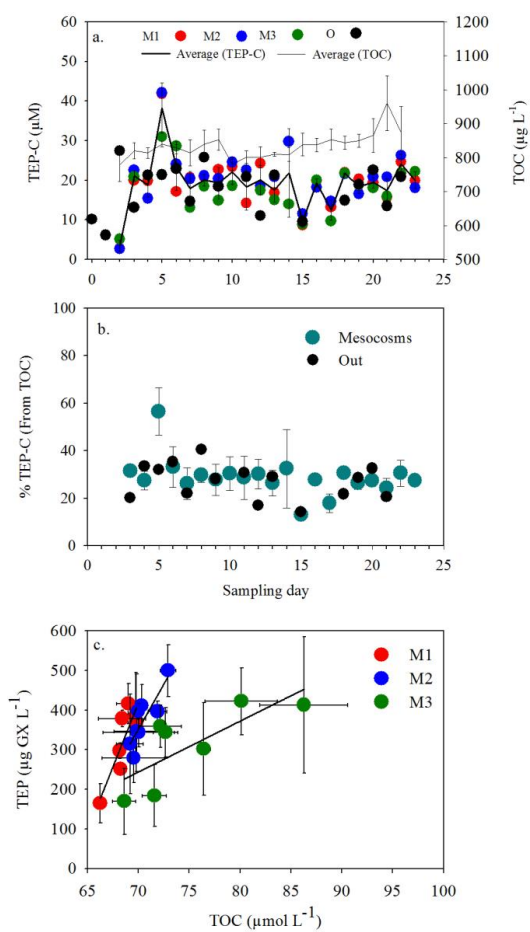
865

866

867 **Figure 4**

868

869



887

888

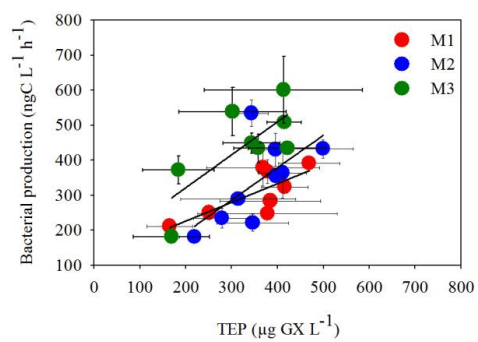
889



890 **Figure 5**

891

892



893

894

895

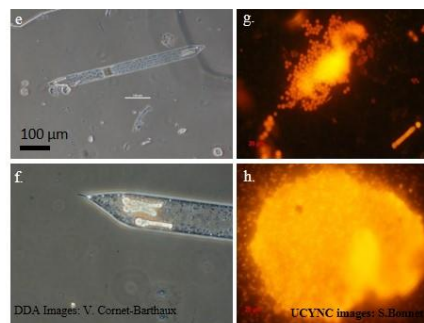
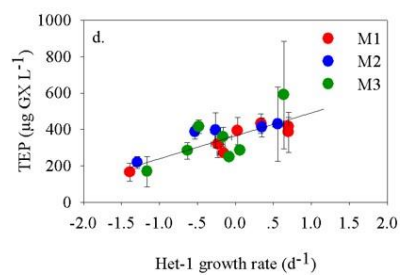
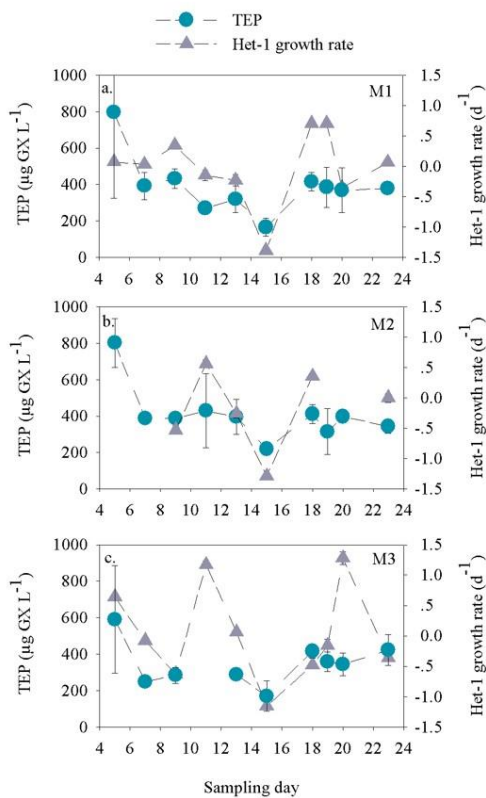
896



897 **Figure 6**

898

899



900

901

902

903

904

905